PROCEEDINGS B

royalsocietypublishing.org/journal/rspb

Research



Cite this article: Aaskov ML, Nelson D, Lauridsen H, Huong DTT, Ishimatsu A, Crossley II DA, Malte H, Bayley M. 2023 Do airbreathing fish suffer branchial oxygen loss in hypoxic water? *Proc. R. Soc. B* **290**: 20231353. https://doi.org/10.1098/rspb.2023.1353

Received: 16 June 2023 Accepted: 18 August 2023

Subject Category:

Development and physiology

Subject Areas:

physiology, evolution

Keywords:

respirometry, cardiovascular bauplan, Pangasionodon hypophthalmus, gill oxygen loss

Author for correspondence:

Magnus L. Aaskov e-mail: magnus.aaskov@bio.au.dk

Electronic supplementary material is available online at https://doi.org/10.6084/m9.figshare. c.6806614.

THE ROYAL SOCIETY

Do air-breathing fish suffer branchial oxygen loss in hypoxic water?

Magnus L. Aaskov¹, Derek Nelson², Henrik Lauridsen³, Do Thi Thanh Huong⁴, Atsushi Ishimatsu⁵, Dane A. Crossley II², Hans Malte¹ and Mark Bayley¹

(ii) MLA, 0000-0001-9458-2854; HL, 0000-0002-8833-4456

In hypoxia, air-breathing fish obtain O₂ from the air but continue to excrete CO₂ into the water. Consequently, it is believed that some O₂ obtained by air-breathing is lost at the gills in hypoxic water. Pangasionodon hypophthalmus is an air-breathing catfish with very large gills from the Mekong River basin where it is cultured in hypoxic ponds. To understand how P. hypophthalmus can maintain high growth in hypoxia with the presumed O2 loss, we quantified respiratory gas exchange in air and water. In severe hypoxia (PO₂:≈ 1.5 mmHg), it lost a mere 4.9% of its aerial O2 uptake, while maintaining aquatic CO2 excretion at 91% of the total. Further, even small elevations in water PO2 rapidly reduced this minor loss. Charting the cardiovascular bauplan across the branchial basket showed four ventral aortas leaving the bulbus arteriosus, with the first and second gill arches draining into the dorsal aorta while the third and fourth gill arches drain into the coeliacomesenteric artery supplying the gut and the highly trabeculated respiratory swim-bladder. Substantial flow changes across these two arterial systems from normoxic to hypoxic water were not found. We conclude that the proposed branchial oxygen loss in air-breathing fish is likely only a minor inefficiency.

1. Introduction

Many teleost fish resort to air-breathing in hypoxic and warm tropical waters and this ability has evolved independently more than 80 times [1]. These multiple appearances have resulted in a variety of air-breathing organs (ABOs), which have typically evolved as modifications or extensions of existing organs [2-4]. The dependence on air-breathing in fish falls along a spectrum ranging from obligate air-breathers that will drown without access to air in normoxic water to facultative air-breathers that may only access the air-phase when water hypoxia is deep enough to prevent sufficient aquatic oxygen uptake [5]. While air-breathing obviously provides access to a plentiful oxygen supply when the fish is residing in hypoxic water, the ABO also requires reorganization of the cardiovascular system to allow adequate perfusion of the respiratory surfaces so that oxygen loading can take place [4-7]. ABOs have been the focus of multiple studies, but the accompanying cardiovascular modifications and their function remain poorly understood. It is generally agreed that irrespective of how an air-breathing fish takes up oxygen it will excrete most of the produced CO2 to the water-phase as a consequence of the much higher CO₂ solubility than O₂ solubility in water [2,8–14]. Thus, it has been argued repeatedly that with the undivided fish heart and associated circulation, airbreathing fish must suffer branchial loss of aerially sourced oxygen when residing in sufficiently hypoxic water [2,3,15-17]. However, it has also been argued that there must be strong selective pressure to reduce this loss because of the importance of oxygen in ATP production [2,18]. Furthermore, it has also been

¹Division of Zoophysiology, Department of Biology, Aarhus University, 8000C Aarhus, Denmark

²Department of Biological Sciences, University of North Texas, 1155 Union Circle, Denton, TX 76203, USA

³Comparative Medicine Lab, Department of Clinical Medicine, Aarhus, Denmark

⁴College of Aquaculture and Fisheries, Can Tho University, Can Tho, Vietnam

⁵Institute for East China Sea Research, Nagasaki University, Nagasaki, Japan

Proc. R. Soc. B 290: 20231353

pointed out that this branchial oxygen loss represents something of a paradox since many of these species are known to show near-endothermic growth rates even when cultured in deeply hypoxic water [19]. Indeed, experimental evidence supporting this oxygen loss hypothesis is limited to few studies, including calculated values from blood flow and blood gas measurements in the bowfin (Amia calva, 7% loss) [15], multiple blood gas samplings in heavily instrumented gar (Lepisosteus oculatus, 10% loss) [16] and water oxygen measurements across the gill basket in armoured catfish (Hypostomus aff. pyreneusi) [17]. In the latter, only four of 11 individuals showed any oxygen loss at all [17]. Reliable measurements in noninstrumented animals have been hampered by the difficulties involved in quantifying CO2 excretion to the water-phase. This difficulty was recently overcome in a study of the airbreathing Arapaima gigas. Here, it was shown that even at a water PO2 of only 1 mmHg where 100% of oxygen uptake was sourced from air, 77% of the produced CO2 was still excreted into the water and that further, there was no evidence of branchial oxygen loss [20]. Arapaima gigas is an obligate airbreather with strongly reduced gills, where the secondary lamellae are almost eliminated in juvenile and adult stages [21]. However, the separation of gas exchange exhibited by A. gigas must require other adaptations that likely include shunting of blood past the gills but also some degree of flow separation of blood streams, through the undivided heart [20]. A reduction of the gills is normally seen as a key adaptation to life in hypoxic water and expected to reduce oxygen loss [2,15,21-23]. So much so, that it has been speculated that the Australian lungfish Neoceratodus forsteri would die in severely hypoxic water because of the branchial O2 loss expected to occur over its well-developed gills [24]. To understand the extent of oxygen loss in air-breathing fish in hypoxic water, direct measurements are clearly needed and since most of the measurements to date have been on obligate air-breathing fish, we deemed it desirable to examine a species on the other end of the obligate-facultative scale with large gills capable of sustaining the oxygen requirements in normoxia.

Pangasianodon hypophthalmus is a facultative aquatic airbreathing teleost native to Southeast Asia [25] that uses its physostomous swim-bladder as its accessory respiratory organ [25–27]. It is the single most cultured air-breathing fish species with an annual global production exceeding 2.5 million tons in 2017 with 94% of this production occurring in Southeast Asia [19] (FAO). Unusual among air-breathers, P. hypophthalmus has a highly active lifestyle and migrates more than 2000 km up the Mekong river system from its feeding to its breeding grounds [28,29] and frequently encounters hypoxic water. The diffusive area of its gills is highly plastic and in normoxic water in situations with low oxygen demand, the effective gill surface area is very small as a result of fully developed inter lamellar cell mass (ILCM) [22]. At elevated water temperatures, in hypoxic water, or during high oxygen demand, the ILCM is shed and the effective gill surface area becomes large with an anatomical diffusion factor exceeding that of many active water-breathing fish [22,30]. Thus, its gills can sustain its entire oxygen demand during exercise in normoxia [31]. Based on these features, we hypothesized that P. hypophthalmus would show branchial oxygen loss in hypoxic water.

The main purpose of this study was therefore to determine the extent of oxygen loss in aquatic hypoxia of P. hypophthalmus and to further understand this oxygen loss by characterizing the morphological and functional characteristics of the cardiovascular system. We quantified the partitioning of oxygen uptake and CO2 excretion in both air- and water-phases allowing measurement of actual branchial O2 loss in deep aquatic hypoxia using a newly developed two-phase respirometer [20]. Further, we charted the circulatory bauplan of P. hypophthalmus with special attention to the branchial basket and modifications for air-breathing using Mercox casts, CT scans with Microfil or barium sulfate and dissections. Finally, we examined the distribution of cardiac output across the branchial basket in surgically recovered fish in normoxia and in deep hypoxia.

2. Material and methods

(a) Experimental animals

Two studies were conducted in Aarhus University, Denmark—a respirometry/branchial O2 loss experiment and a blood flow experiment. The fish used were obtained from Credo Fish (Denmark) and raised from fry to the desired size in 1000 l tanks in a recirculating system at 27°C with a natural light: dark cycle (approx. 11.5:12.5 h), and fed on weekdays with commercial food pellets. Before all measurements, fish were fasted for at least 72 h. The respirometry/branchial O2 experiment was performed on seven individual P. hypophthalmus (mean ± s.d.: 1050 ± 340 g) exposed to normoxia followed by hypoxia and four individuals (mean \pm s.d.: 1009 ± 175 g) exposed to normoxia followed by normoxia to control for possible habituation to the respirometer. For the blood flow experiment fish were 363.3 ± 35.7 g (N = 7). All procedures were conducted according to the guidelines of the Danish Law on Animal Experiments and approved by the Danish Ministry of Food, Agriculture and Fisheries (2016-15-0201-00865).

For the investigations of cardiovascular layout, fish were obtained from local farmers near Can Tho University in Vietnam and after preparation, the filled carcasses were transferred to Nagasaki Japan or Aarhus University, Denmark for analysis. These animals had a mean body mass of 820 ± 53 g.

(b) Respirometry methods

The respirometer and methods have previously been described in detail in [20]. The respirometer used was a water-filled cylinder (30.1 l) with a small air-filled chamber (≈800 ml) at the top of one end.

(i) Experimental protocol

Fish were placed in the respirometer maintained at 31°C in normoxic water and allowed to acclimatize to the respirometer for 21 h before measurements started. Four fish were then exposed to a protocol of two successive periods of normoxic water of duration 20 h each to determine any possible signs of habituation to the respirometer. Seven further fish were exposed to a protocol consisting of a 20 h period of normoxia (PO₂: 114.77 ± 10.78 mmHg, mean \pm s.d.) followed by a 20 h period of hypoxia (PO₂: 1.5 \pm 0.82 mmHg, mean \pm s.d.) (electronic supplementary material, figure S1). Since the fish reacted strongly to sudden hypoxia, the first closed measurement loop in the hypoxia period was deliberately milder with starting PO₂ ranging from 37.5 to 62 mmHg to ensure that the fish initiated air-breathing before aquatic O2 uptake became impossible. After the hypoxia measurements, the fish was removed and weighed, and background measurements performed to estimate both the bacterial gas exchange (normoxia) and the extent of diffusion of O₂ between phases (severe aquatic hypoxia). Diffusion of O₂ from the sealed air chamber into the water during the 15 min flush period was also measured after each replicate. Aerial PO₂ and PCO₂ gas analysers were calibrated before each trial.

Table 1. Equations used in this study with explanations.

equations respirometry	abbreviations and explanations		
aquatic oxygen uptake (MO ₂):	$\Delta PO_2=$ change in PO_2 during a measurement period		
$\dot{M}_{0_2} = \frac{(\Delta PO_2 - \Delta PO_{2_bacteria}/\Delta t)*\beta O_2*V_{sys}}{M_b} $ (2.1)	$\Delta PO_{2_bacteria} = bacterial \ O_2$ use		
	$\Delta t =$ length of a closed measurement period (20 min)		
	$\beta 0_2 = 0_2$ solubility at 31°C		
	$V_{\text{sys}} = \text{water volume of respirometer minus fish volume}$		
	$M_b = \text{body mass of fish}$		
aquatic CO ₂ excretion (MCO ₂):	β CO ₂ = CO ₂ solubility at 31°C		
amount injected:	$P = total gas pressure (atmospheric pressure minus water vapour pressure ($\approx760-$		
$CO_{2_injected} = \beta CO_2 * P * V (2.2)$	33 mmHg)		
	$V =$ known volume of CO_2 -saturated distilled water		
calibration factor:	$\int_0^T CO_{2,bacteria} = AUC$ for CO_2 of background measurement		
$CO_{2,calibration} = \frac{CO_{2,injected}}{\int_0^T CO_{2,measured} - \int_0^T CO_{2,bacteria}} $ (2.3)	$\int_0^T CO_{2,measured} = Area under curve (AUC) for CO_2$		
CO ₂ accumulated per period (MCO ₂): $CO_{2,\text{calibration}} * \left(\int_0^T CO_{2,\text{measured}} - \int_0^T CO_{2,\text{bacteria}} \right) \qquad (2.4)$	T= time of measurements period. In this case, the 20 min closed water period of the chamber		
nerial O ₂ uptake	$\dot{V}=$ is the air flow rate		
$\dot{M}O_2 = \dot{V} * \int_0^T (F_{\text{baseline}} - F_{O_2}(t)) dt$ (2.5)	$\int_0^T = AUC$ between O_2 or CO_2 and baseline		
nerial CO ₂	$F =$ fractional concentration of O_2 or CO_2		
$\dot{M}CO_2 = \dot{V} * \int_0^7 (F_{CO_2}(t) - F_{baseline}) dt$ (2.6)	baseline = the $\%$ inflow concentration of either O_2 or CO_2		
	T= time of measurement period (20 min with open flow $+$ 15 min accumulated use during flush period)		
nstantaneous volume equation (Q)	V = measured voltage		
$Q \text{ (L min}^{-1}) = (V*D^2)/(271.2*\cos A)$ (2.7)	D = probe diameter		
	A = angle of the crystal (45°)		

(ii) Timing of measurements

The air- and water-phases were, by necessity, not flushed simultaneously because doing so resulted in flooding of the air-space. A measuring loop lasting 35 min was therefore divided into two periods: a 20 min 'open air-phase with closed water-phase' (closed water) period and a 15 min 'closed air-phase with open water-phase' (flush) period. Aquatic PO2 was measured during the 20 min closed water period and water conditions were replenished during the 15 min flush period (aquatic PO₂ measured 20 out of 35 min). The aerial gas exchange that accumulated in the sealed air chamber during the 15 min water flush period was measured together with the gas exchange during the following 20 min closed water period. Hence, the entirety of gas exchange to the air was measured during a 35 min cycle, whereas for the water-phase 20 of the total 35 min were measured (see electronic supplementary material, figure S2).

(iii) Water CO₂ excretion—intermittent closed respirometry

The aquatically excreted CO₂ was measured using a method closely resembling that described in [32]. During every 20 min closed water period, all the CO₂ excreted into the water accumulated in the water. Then during the 15 min flush phase, the chamber water was flushed out of the respirometer through an artificial lung (Affinity Fusion Oxygenator BB811, Medtronic Inc. Technology, UK) where CO₂ was transferred via diffusion from the respirometer water to a carrier gas (N₂) and measured with an infrared CO₂ analyser (LI-830 CO₂ Gas Analyser, LI-COR Biosciences, Lincoln, NE, USA). The artificial lung consists

of microporous polypropylene hollow fibre membranes resulting in a large surface area (2.5 m^2) where the carrier gas runs countercurrent to the water optimizing the exchange. The extraction of CO_2 from the water was calibrated by injecting known volumes of CO_2 -saturated, distilled water (equations (2.2)–(2.4), table 1) into the respirometer during a closed loop. These injections were made after removal of the fish from the chamber and followed the normal protocol timings to include bacterial CO_2 production. The injections were made at the start of a closed loop to ensure the injected CO_2 was fully mixed with the respirometer water before extraction through the lung.

(iv) Water-phase O₂ uptake-intermittent closed respirometry

Aquatic MO₂ was measured using intermittent closed respirometry as described previously [26,33] and calculated using equation (2.1) in table 1. PO₂ was measured with a Hamilton O₂ optode (Visifirm DO, Hamilton Company, Bonaduz, Switzerland) in a closed circulation loop. The respirometer was submerged in water in an aquarium to maintain a stable temperature and this outer aquarium covered in dark plastic to minimize visual disturbance. The air chamber at the front of the respirometer was left uncovered so that the air-phase was lit up for the fish. Water was made hypoxic by bubbling a header tank (≈200 l, 0.4 mmHg, surface covered with Astro foil) with N2 while PO2 was monitored by a Hamilton O2 optode. The respirometer chamber water was flushed back into the header tank since at least 901 of water (chamber volume *3) was exchanged during each flush period. Normoxic water was vigorously bubbled with air in a header tank to keep water close to saturation (greater than 90% saturation). Full saturation was not

possible because the artificial lung was very efficient at removing CO_2 but also O_2 since we used pure N_2 as the carrier gas. Temperature, PO_2 logging, and start/end of flush periods was automated by using an in-house made relay and software system (Respirometer 2.0, Zoophysiology, Aarhus University).

(v) Air-phase—intermittent closed respirometry

Aerial O2 uptake and aerial CO2 excretion was measured using intermittent closed respirometry in normoxic and normocapnic air and analysed using equations (2.5) and (2.6) (table 1). During the sealed phase in severe hypoxia, PO_2 dropped to $136.9\,\pm$ 5~mmHg and PCO2 rose to $1.2\pm0.4~\text{mmHg}.$ Diffusion of O2 from the sealed air chamber during the 15-flush period was estimated using equation (2.5) after the fish was removed (integral of the deviation from O2 baseline in subsequent closed period). Air was passed through a drying column (CaCl₂) and O₂ and CO₂ fractional concentrations were measured using a FC-10 Oxygen Analyzer (Sable Systems, GmbH) and a CA-10 Carbon Dioxide Analyzer (Sable Systems, GmbH). Data were logged with a MP100 data acquisition system (Biopac System Inc., Goleta, CA, USA) connected to a computer running Acqknowledge (v.3.9 Biopac systems). Airflow was controlled by a suction pump (FlowControl R2, Applied electrochemistry, Pittsburg, PA, USA) and the airflow rate was measured continuously using a mass flow meter (Sierra 830D-L-1-V1, Sierra Instruments, CA, USA).

(c) Methods for the anatomical descriptions of the circulation

The circulatory anatomy was investigated visually by filling the vasculature with a methylmethacrylate-based resin (Mercox) and dissolving the surrounding tissue using a strong base and by micro-CT imaging after filling the vasculature with a liquid containing a radio-opaque chemical (barium sulfate or Microfil (MV-122, Flowtech-Inc, Boulder, CO)). In addition, two fish were injected after anaesthesia with Evans blue to allow visual inspection of the vasculature during dissection. For Mercox casting, fish were anaesthetized in water containing benzocaine (1.5 g l⁻¹) and the bulbus arteriosus was cannulated with a catheter (Hibiki no. 7, Kunii, Tokyo). The blood was flushed out using heparinized saline (50 IU ml⁻¹) and the cardiovascular system was filled with Mercox using a hand-controlled pump [33]. The tissue was macerated in alternative baths of 20% NaOH and 2% HCl, after which the cast was rinsed exposing the fine net of the vascular system for examination.

(i) Barium sulphate casting

The same cannulation and anaesthetic procedure were used. Two fish where placed in a 40°C water bath, blood was washed out with heparinized saline saturated with sodium nitroprusside to induce vasodilation and filled with barium sulfate in saline (20–30%) and gelatin (5%) [34]. The cast was scanned in a micro-CT scanner (Scanco Xtreme) using a $82\times82\times82~\mu\text{m}^3$ resolution at 60~kV and $900~\mu\text{A}$ with a 65~min acquisition time. Pictures were assessed in the program Osiris.

(ii) Microfil casting

The same procedure as for the barium sulfate protocol, but fish were filled with a diluted solution of yellow Microfil (protocol II in Zhou *et al.* [35]) using a 10% MV Curing Agent concentration. The cast was micro-CT scanned and analysed as above.

(d) Blood flow measurements

Seven fish $(363.3 \pm 35.7 \text{ g})$ were fasted 24 h before surgical instrumentation. Animals were anaesthetized with benzocaine (120 mg l^{-1}) until motor reflexes were abolished, approximately

5 min. The animal was then transferred to a surgical tray allowing the gills to be irrigated with an oxygenated maintenance solution of benzocaine (37.5 mg l⁻¹) until surgery was completed. The left operculum and gills were retracted to expose the thin epithelium lining on the left side of the isthmus. A centimetre incision was made starting 0.5 cm up from the ventral surface and 0.5 cm caudal from the origin of the operculum. Based on the vascular casting studies the ventral aorta was exposed under a dissection microscope immediately after leaving the bulbus arteriosus and identified as; ventral aorta one (VA1) situated on a horizontal plane, ventral aorta two (VA2) at a 45° angle (two total, one on each side) and a combined ventral aorta supplying gill arches three and four (VA3/4) on a vertical plane. VA1 and VA3/4 were separated from connective tissue and fitted with Doppler flow probes, 1.3 mm and 1.6 mm, respectively (Iowa Doppler Products). The leads were anchored with silk suture to the isthmus, along the cleithrum and just rostral of the dorsal fin. Animals were immediately transferred to a bimodal swim tunnel, containing a freshwater and an air-phase with water flow rate set at 0.5 body lengths s⁻¹ and temperature maintained at 31°C. Astro foil was used to cover the swim tunnel preventing disturbances and reducing ambient air-water interface. Animals were left undisturbed for 24 h to recover from the surgical procedures.

After recovery, fish were progressively exposed to hypoxia by bubbling nitrogen gas into the water-phase (PwO2: approx. 145 mmHg to less than 10 mmHg) of the swim tunnel for a minimum of 100 min. The air-phase was accessible to ambient air (PO $_{\!2}\!\sim\!145\,\text{mmHg}).$ PO $_{\!2w}$ was measured with a Hamilton $O_{\!2}$ optode. Doppler flow probe leads were connected to a directional pulsed Doppler blood flow meter (Model 545C-4, Bioengineering, University of Iowa, Iowa City, IA, USA) and recorded at 100 Hz using a PowerLab16/35 data acquisition system (ADInstruments, Colorado, USA) and subsequently analysed using LabChart data acquisition software (Chart 8.1, ADInstruments). The blood flow response was determined as the mean values in two 5 min samples collected for each animal during the normoxic exposure 5 min before starting the hypoxia protocol and at least an hour after $P_w O_2$ reached less than 10 mmHg. Subsequently, animals were euthanized by an overdose of benzocaine and blood flow in each vessel was measured to calibrate for zero flow.

(e) Data analysis

(i) Respirometry data

Aquatic, aerial and total MO₂, MCO₂ and respiratory exchange ratio (RER) were calculated for each loop. SMR was calculated from MO₂ time series using the 10% quantile method from the R script in [36] and compared with a two-tailed Student's *t*-test. The first measurement loop was omitted for all normoxia measurements since the oxygenator was not in equilibrium with the water during the first loop. Respirometry data (table 2) were analysed using linear mixed models in R (lme4 package [37]) to account for the repeated measures in fish. We used a random slope model with Treatment (normoxia/severe hypoxia) as a fixed effect and Fish a random effect. To test for significance (level: 0.05) a post-hoc analysis was completed in R using *postHoc* [38], which uses a semiparametric test where *p*-values for the pairwise comparisons are corrected using the single-step method from [39].

(ii) Blood flow data and heart rate

Heart rate ($f_{\rm H}$) was calculated from the blood flow pulse interval (average rate during 300 s). Mean blood flows (Q), from VA1 ($Q_{\rm VA1}$) and VA3/4 ($Q_{\rm VA3}$) were calculated with the instantaneous volume equation (equation (2.7) (table 1)—[40]). Maximum ($Q_{\rm maxVA1}$) and minimum ($Q_{\rm minVA3}$) blood flow of both aortas were taken during systolic and diastolic phases of the cardiac

Table 2. Respirometric measurements of 0_2 uptake and CO_2 excretion in both water and air in normoxia (N = 7) and severe hypoxia (N = 7). Last two columns show habituation—normoxia measurements (N = 4). Data are presented as average values \pm s.e. Uptake and excretions are expressed as μ mol min⁻¹ kg⁻¹ while O_2 loss and partitioning of uptake/excretion from air is expressed as a percentage of total. *Significant difference between treatments (p < 0.05). (Data were only compared within groups—normoxia with severe hypoxia and habituation—normoxia with habituation—normoxia 2.) RER, respiratory exchange ratio.

	normoxia	severe hypoxia	habituation-normoxia	habituation-normoxia 2
$\mathrm{MO}_{\mathrm{2air}}~(\mu\mathrm{mol~min}^{-1}~\mathrm{kg}^{-1})$	4.69 ± 0.53	66.86 ± 4.35 *	3.22 ± 0.47	3.61 ± 0.71
MO_{2water} (µmol min ⁻¹ kg ¹)	61.10 ± 3.91	-3.36 ± 0.68 *	65.36 ± 6.04	58.92 ± 5.04
MO_{2use} (μ mol min ⁻¹ kg ⁻¹)	65.80 ± 4.21	63.46 ± 4.32	68.60 ± 6.3	62.54 ± 4.50
MCO_{2air} (µmol min ⁻¹ kg ⁻¹)	0.47 ± 0.07	4.43 ± 0.76*	0.466 ± 0.05	0.422 ± 0.03
MCO_{2water} (µmol min ⁻¹ kg ⁻¹)	60.88 ± 4.11	48.15 ± 4.72*	71.98 ± 8.09	63.07 ± 5.29*
MCO _{2total} (μmol min ⁻¹ kg ¹)	61.34 ± 4.27	52.53 ± 5.07*	72.43 ± 8.13	63.49 ± 5.31*
percentage aerial MO ₂	7.25 ± 0.59	105.40 ± 0.76 *	4.8 ± 0.61	6.05 ± 1.41
percentage aerial MCO ₂	0.80 ± 0.11	8.56 ± 1.06*	0.65 ± 0.04	0.69 ± 0.04 *
RER air	0.11 ± 0.016	$0.06 \pm 0.008*$	0.16 ± 0.03	0.13 ± 0.02
RER water	0.99 ± 0.44	-18.32 ± 4.55 *	1.09 ± 0.05	1.07 ± 0.02
RER total	0.93 ± 0.024	0.82 ± 0.058*	1.05 ± 0.05	1.01 ± 0.02
SMR (µmol min ⁻¹ kg ⁻¹)	54.67 ± 1.65	54.58 ± 3.03	56.07 ± 6.26	51.86 ± 3.96
branchial O ₂ loss (% of SMR)		6.07 ± 0.91		
branchial O ₂ loss (% of aerial uptake)		4.92 ± 0.67		

cycle, respectively. All blood flow values were corrected for mass. Blood flow and $f_{\rm H}$ data were analysed with repeated measures ANOVA with $P_{\rm w}O_2$ as the dependent variable. For flow data a repeated measures ANOVA with $P_{\rm w}O_2$ as the dependent variable and vessel type being the independent variable was used. ANOVA tests were followed by an LSD post-hoc test to compare individual means (p < 0.05) (Statistica 13.0; TIBCO software Inc., Palo Alto, CA, USA).

(iii) Calculation equations

See table 1 for calculation equations used in this study.

3. Results

(a) Bimodal respiration

Total O2 uptake did not differ significantly between normoxia and hypoxia treatments (p-value: 0.67); however, the mode of breathing changed as expected of a facultative airbreathing fish. Aerial O₂ uptake changed from 7.25% in normoxic water to 105.4% of total O₂ use in hypoxic water. Aerial uptake exceeds 100% because the fish takes up enough oxygen to cover both its metabolic usage and the small amount of branchial loss to the hypoxic water. The partitioning of CO₂ excretion differed less than the partitioning of O2 since most of the CO2 was excreted into the water in both normoxia (99.2%) and severe hypoxia (91.44%). Total CO₂ excretion differed significantly between treatments, as it was 14% lower in the second (severe hypoxia) measurement period compared to the first (table 2, figure 1). A similar pattern was seen in the habituation control group where the total CO₂ excretion in the second normoxia treatment was 12% lower than the first (electronic supplementary material, figure S3). A regression analysis showed that the aerial CO2 excretion during hypoxia increased with time while the aquatic excretion remained constant (p-values: 0.03 and 0.14). Bacterial O2 consumption in normoxia was $2.05 \pm 0.83\%$ (mean \pm s.d.) of the fish oxygen uptake and was subtracted for oxygen uptake calculations.

(b) Branchial O₂ loss

All seven fish experienced a branchial O_2 loss during severe hypoxia averaging $4.92 \pm 0.67\%$ of aerial uptake at an average PO_2 of 1.5 ± 0.82 mmHg (figure 2). This loss varied between fish (average loss as percentage of SMR: 2.14% for lowest and 10.00% highest) and remained throughout the hypoxia exposure. The initial higher water PO_2 occurred because the first flush returned the less hypoxic water from the chamber to the severe hypoxic header tank, which initially increased the PO_2 in the header tank. This resulted in a PO_2 of 4.71 ± 1.12 mmHg in the first severe hypoxia measurement loop and the branchial loss was only $3.6 \pm 0.5\%$.

(c) Cardiovascular system in *Pangasionodon* hypophthalmus

The combined data from our investigative approaches was used to map the circulatory system. The heart is located ventrally and posterior to the gills in a bony cavity. Blood from the heart flows through the bulbus arteriosus and into four different ventral aortas (figure 3). The first ventral aorta (VA1) leaves the bulbous arteriosus in the horizontal plane, splits in two shortly thereafter, to supply the first left and right branchial arches. Two ventral aortas (VA2L and VA2R, 45° angle) lie immediately dorsal to VA1 and feed the second left and right branchial arch, respectively. The last and biggest ventral aorta (VA3/4, vertical plane) courses anterodorsally and splits twice, first into left and right and second to supplying the third and fourth branchial arches. The efferent branchial arteries from the branchial arches feed different vessels: arteries from the first and second gill arches form the dorsal aorta (DA) supplying the head and trunk while arteries from the third and fourth gill arches

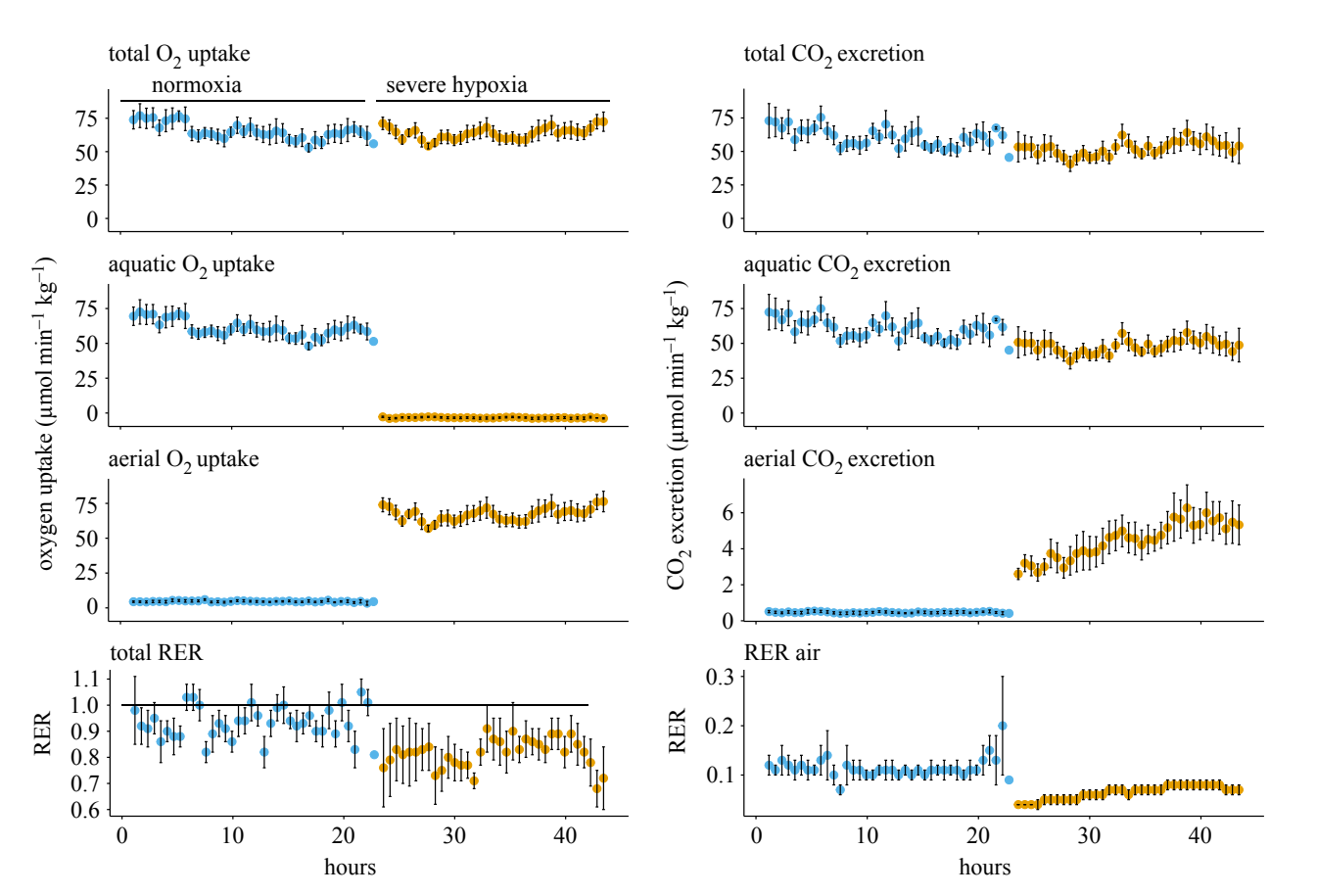


Figure 1. The mean mass-specific rates for O₂ uptake, CO₂ excretion and RER in both water and air in normoxia and severe hypoxia. Each dot shows a measurement period and blue dots represent normoxia while orange dots represent severe hypoxia (N = 7, 1050 \pm 340 g, all fish experienced both treatments starting with normoxia). Mean \pm s.e. shown. The line in total RER (respiratory exchange ratio) shows RER = 1.

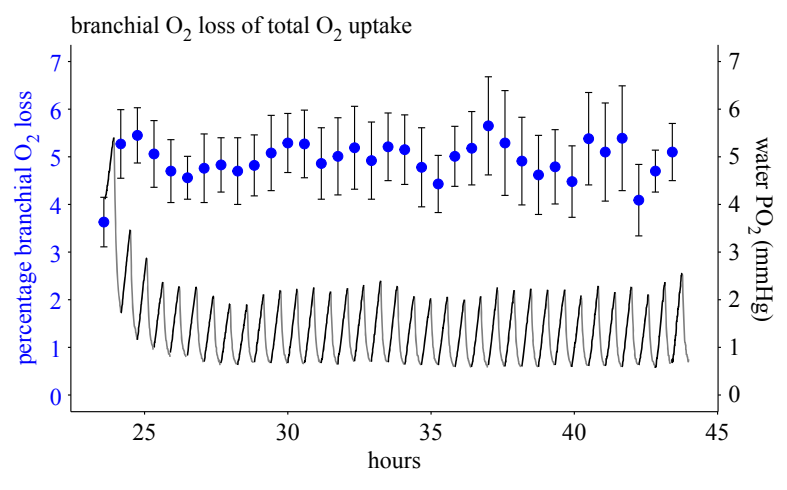


Figure 2. The mean branchial O_2 loss as a percentage of the total O_2 uptake, and the water PO_2 during the measurements (N = 7). Each blue dot represents the mean percentage lost during the corresponding 20 min period with s.e. The black lines shows the average (all fish) PO₂ of the water (right y-axis) with approximately two measurements per minute during the 20 min period. A positive slope is, therefore, equal to the O₂ loss from the fish. The grey lines show the PO₂ during the 15 min flush periods (right axis).

form the coeliacomesenteric artery (CMA) supplying the gut and gas bladder artery (GBA) that supplies the ABO. The ABO is highly vascularized with numerous trabeculae and has a large central artery (ABO artery) running centrally with frequent branching to form a dense capillary network. The DA and CMA are joined by a post-branchial anastomosis. This anastamosis was missing from the barium sulfate and Microfil fills, but was consistently found in Mercox fillings and during dissection. This vessel responded to pharmaceutical injections, which indicated that blood flow

between the DA and CMA can be regulated (see electronic supplementary material, information).

The venous circulation could only be adequately filled using Evans blue, which has a lower viscosity than barium sulfate, Mercox and Microfil. Evans blue coloured the circulation during dissection and revealed that the ABO is drained through the ABO vein running in close parallel to the ABO artery. The ABO vein exits the ABO and passes through the head kidney before merging with the hepatic vein shortly before the hepatic vein opens into the sinus venosus.

Proc. R. Soc. B 290: 20231353

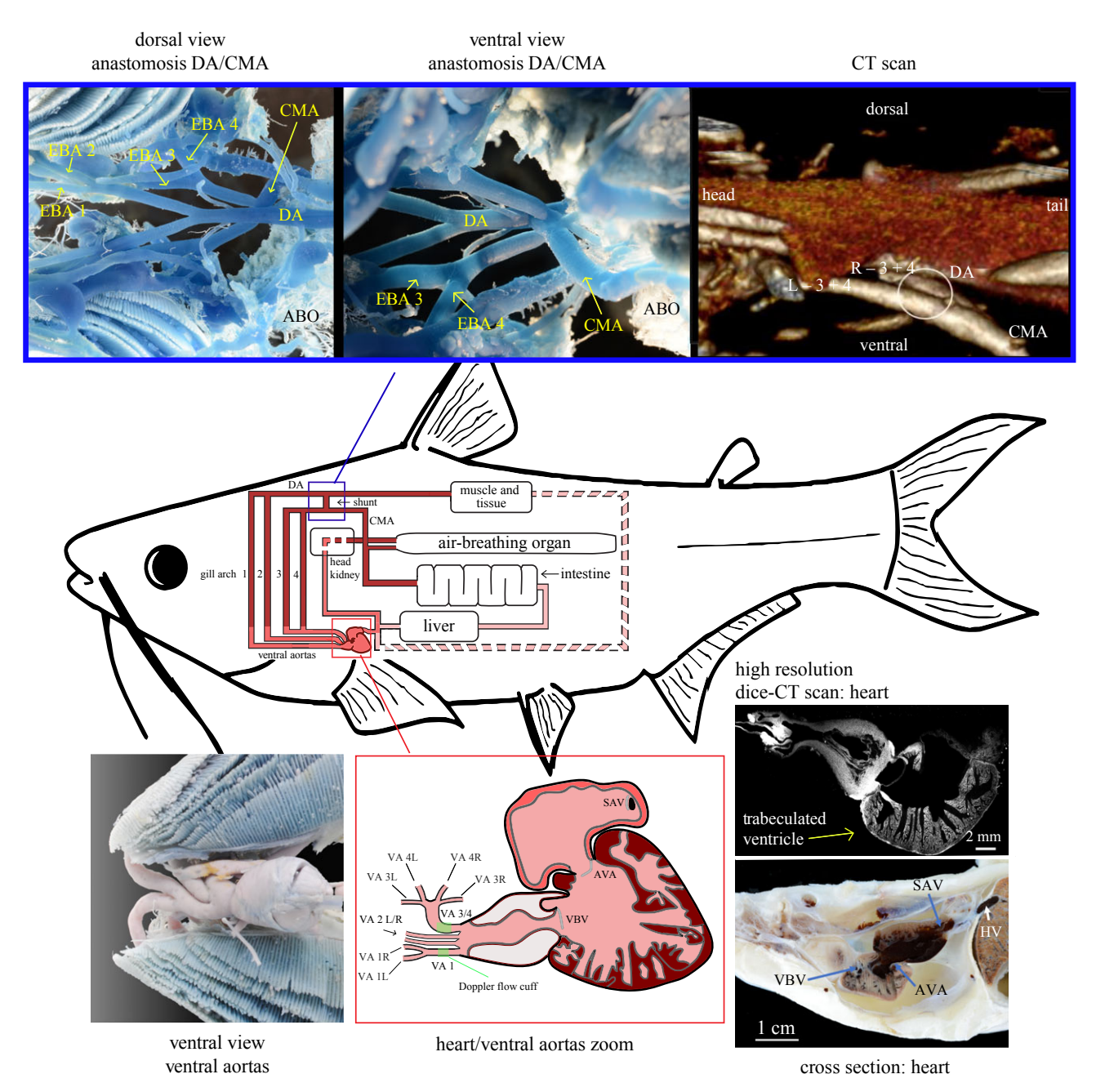


Figure 3. A simplified version of the cardiovascular system in *P. hypophthalmus* with focus on the ventral aortas and the shunt/anastomosis of dorsal aorta and coeliacomesenteric artery. DA, dorsal aorta; CMA, coeliacomesenteric artery; EBA, efferent branchial artery; ABO, air-breathing organ; VA, ventral aorta; L/R, left/right; HV, hepatic vein; SAV, sinoatrial valve; AVA, atrioventricular valve; VBV, ventriculobulbar or semilunar valve. The ventral aortas are named after which gill arch they supply and when they split, which side they supply.

Dissection of the heart revealed a very trabeculated ventricle and valves between the sinus venosus and atrium, the atrium and ventricle, and the ventricle and bulbus arteriosus.

(d) *In vivo* flow measurements

Blood flows and $f_{\rm H^-}$ were measured during normoxia ($P_{\rm w}O_2$ = ~144 mmHg) and hypoxia ($P_{\rm w}O_2$ = ~10 mmHg) while swimming slowly at 0.5 body lengths s⁻¹.

Mean blood flow (*Q*) increased significantly following the transition from normoxia to hypoxia in VA 3/4 (normoxia: $15.30 \pm 2.99 \,\mathrm{ml\ min^{-1}\ kg^{-1}}$, hypoxia: $24.88 \pm 3.22 \,\mathrm{ml\ min^{-1}\ kg^{-1}}$) while in the increase seen in VA 1 (normoxia: $6.91 \pm 1.03 \,\mathrm{ml\ min^{-1}\ kg^{-1}}$, hypoxia: $9.90 \pm 2.06 \,\mathrm{ml\ min^{-1}\ kg^{-1}}$) was less pronounced and not significant. The systolic blood flow (Q_{max}) also increased

significantly transitioning from normoxia to hypoxia in VA 3/4 (normoxia: 25.88 ± 3.64 ml min⁻¹ kg⁻¹, hypoxia: 33.99 ± 3.47 ml min⁻¹ kg⁻¹) while more or less unchanged in VA 1 (normoxia: 15.36 ± 2.24 ml min⁻¹ kg⁻¹, hypoxia: 19.46 ± 4.29 ml min⁻¹ kg⁻¹). Diastolic blood flow ($Q_{\rm min}$) showed the same pattern being significantly different for VA 3/4 (normoxia: 8.52 ± 2.75 ml min⁻¹ kg⁻¹, hypoxia: 17.05 ± 3.52 ml min⁻¹ kg⁻¹) but not for VA 1 (normoxia: 0.73 ± 1.17 ml min⁻¹ kg⁻¹, hypoxia: 3.52 ± 1.32 ml min⁻¹ kg⁻¹).

No Doppler probes were placed on VA2 L/R, making it challenging to compare blood flow rates. However, since the DA is supplied by VA1 and VA2, while the CMA is supplied by VA3/4, then by assuming comparable flows through VA1 and VA2, our results indicate comparable flows through the DA and CMA between treatments (normoxia: Q DA: $6.91 \times 2 = 13.8$, Q CMA = 15.30, hypoxia: Q DA: $9.9 \times 2 = 13.8$

Figure 4. The heart rate and values of blood flow in *P. hypophthalmus*. (*a*) Max heart rate, (*b*) average blood flows (*Q*), (*c*) minimum blood flow (Q_{min}) and (*d*) maximum blood flow (Q_{max}) in ventral aorta one (VA1) and the pre-split ventral aorta three and four (VA3/4). A white bar = normoxia and a black bar = hypoxia. Different letters (a, b) indicates a significant difference between normoxia and hypoxia (p < 0.05). N = 7 for all and values are mean \pm s.e.

19.8, Q CMA = 24.88). During normoxia $f_{\rm H}$ was 101 ± 5 beats min⁻¹ and increased significantly to 142 ± 7 beats min⁻¹ during hypoxia (figure 4d).

4. Discussion

Downloaded from https://royalsocietypublishing.org/ on 13 September 2023

We found that P. hypophthalmus suffered only limited oxygen loss in deep hypoxia at $PO_2 < 2$ mmHg amounting to an average 4.9% of the oxygen uptake. This was a surprisingly small fraction of the total oxygen uptake given that under these conditions 91% of the CO_2 produced was excreted into the water-phase.

When transitioning from normoxia to severe hypoxia P. hypophthalmus changes from a water-breather (93% aquatic uptake) to a complete air-breather with regard to O2 uptake. The aquatic CO₂ excretion fraction, however, only changes from 99% in normoxia to 91% during severe hypoxia. This continuous aquatic CO2 excretion in severe aquatic hypoxia has also been reported in A. gigas [20] (aquatic $PO_2 \approx$ 1.1 mmHg), L. oculatus [16] ($PO_2 = 12 \text{ mmHg}$), Anabas testudineus [41] ($PO_2 = 2.7-7.5$ mmHg) and in Ancistrus chagresi [42] (PO₂: 5-20 mmHg) as well as a host of other species where only CO₂ excretion to the air-phase was measured (table 5.7 in [2]). Since CO2 is continuously excreted into the water in the current study, blood must come into near contact with the water, most notably during branchial passage, and the anatomical diffusion factor (ADF) of the gills of this species under these conditions can be expected to be very large and comparable to active water breathers such as rainbow trout [30]. Oxygen loss in aquatic hypoxia (PO₂ average 1.5 mmHg) was relatively constant over time averaging $4.9 \pm$ 0.67% of uptake (average ± s.e.) with an inter-individual variation ranging from $1.9 \pm 0.1\%$ to $7.7 \pm 0.2\%$. Interestingly, in the first respirometer flush where hypoxia only reached a PO_2 of 4.71 mmHg, oxygen loss was correspondingly reduced to only $3.6 \pm 0.5\%$ of oxygen uptake. If this experiment had been conducted at higher temperatures or in a swimming-respirometer close to the maximum aerobic swimming speed, the branchial loss could potentially increase as it has been shown that ILCM can only be completely removed during swimming [30]. Phuong *et al.* [30] found that the ADF in resting fish going from 27°C to 33°C was increased by 26%. However, by swimming the animals close to their maximal aerobic speed at 33°C caused an increase in ADF of more than 400%. This might be relevant during the reproductive migrations undertaken by *P. hypophthalmus*. On the other hand, we judge that the chance of encountering deep hypoxia in a well-mixed river system is low.

A telemetry study in a typical Vietnamese aquaculture pond (3000 m², 4 m deep) showed that P. hypophthalmus stays near the top layers of the pond [43]. The study was performed twice in the growth cycle, once early on with fish of 200-500 g and later near harvest with fish approximating 800 g. In the early study, fish mostly stayed almost exclusively in the top 1 m of the pond while those measured close to harvest stayed in the top 0.45 m [43], and the authors suggested that the difference was due to the reduced oxygen saturation in the ponds with the higher biomass. Damsgaard et al. [44] measured the PO2 in the same as well as in other P. hypophthalmus aquaculture ponds (0.400-1 kg fish) to be ≈20, 17 and 8 mmHg at 1, 2.5 and 3 m depths, respectively [44, fig. S1]. We, therefore, expect branchial O₂ loss in freeswimming animals to be substantially less than the present study or even completely absent. In their natural habitat, which is the main body of the Mekong river system [29], P. hypophthalmus would likely only ever encounter such deep hypoxia for very short periods. However, even in

anoxia, these fish will still only lose a small fraction of their O_2 intake (during non-strenuous exercise), despite excreting almost all produced CO_2 to the water.

There are a variety of factors that might contribute to explaining the separation in gas exchange we document here. These include specialized cardiovascular arrangements, the difference in water solubility of CO2 and O2, gill ventilation and perfusion modulation as well as the O2 affinity of the blood. Firstly, at 31°C, CO₂ is approximately 25 times more soluble in water than O2 and, therefore, Krogh's diffusion constant (K) is 20-25 times higher for CO₂ [45] than for oxygen. Secondly, in normoxia and hypoxia the branchial ventilatory drive is controlled by the O2 requirement [46] which results in a hyperventilation with respect to the CO₂ excretion requirement [8]. However, in severe hypoxia facultative air-breathers reduce both the amplitude and frequency of gill ventilation [16,47,48]. This has also been shown in P. hypophthalmus [25]. A lower gill ventilation, at constant CO₂ production, would result in a higher blood PCO₂ (respiratory acidosis). This is indeed indicated in our data, where aerial CO₂ excretion increases slowly during the hypoxia exposure and the aquatic CO₂ excretion is slightly reduced. Whether the changes in CO2 excretion have reached a new steady state at the end of the measurement is unclear without accompanying blood pH and ions and gill ventilation data because the shift to hypoxia also causes a reduction in RER from 0.93 in normoxia to 0.82 in hypoxia with no clear sign of recovery (figure 1). There is no sign of reduced oxygen uptake (metabolic depression) (figure 1). So, this altered RER could be either be a result of altered substrate usage (e.g. a shift towards greater reliance on fatty acids) or a retention of total CO₂ because of incomplete pH regulation requiring an increase in blood bicarbonate that may take significant time to complete [44,49]. Thirdly, a high Hb O_2 affinity (low P_{50}) allows for a greatly reduced oxygen gradient between blood and water without significant unloading of O2 from the haemoglobin during branchial passage. Since the oxygen affinity of most haemoglobins is temperature dependent, with increased affinity at reduced temperatures, it is to be expected that O₂ loss itself would be temperature dependent. This is particularly the case in P. hypophthalmus because of the lack of chloride binding to haemoglobin giving rise to a very large temperature effect and blood oxygen affinity in this species is reduced by 1.71 mmHg/°C [50]. It has previously been shown that facultative air-breathing fish (without transbranchial shunts) have higher O₂ affinities than obligate air-breathers [4], and suggested that the low P_{50} protect against O_2 loss [51].

Our anatomical findings indicate the circulatory bauplan of P. hypophthalmus differs from all the air-breathing fish species described in reviews [5-7]. However, it partly resembles that of snakehead (Channa sp.) with multiple ventral aortas [52,53], and partly the jeju, Hoplerythrinus unitaeniatus, where the first and second gill arches form the DA, while third and fourth forms the CMA, which then has a branch that supplies the ABO [54]. There is also a connection present between the DA and CMA, which resembles the arrangement in the true lungfishes [55]. Hence, this cardiovascular arrangement might allow for the regulation of flow distribution across the branchial basket where blood could be directed towards the first and second gill arches that are most directly connected to the DA, or to the third and fourth gill arches, most directly connected to the CMA and the ABO. For this type of arrangement to lead to the separation of gas exchange sites would in addition require flow separation of oxygenated and de-oxygenated streams.

The heart of *P. hypophthalmus* is strongly trabeculated. A highly trabeculated ventricle has also been observed in *C. argus* [52], *A. gigas* [56,57], and in the amphibian heart. Furthermore, the bulbus arteriosus of *A. gigas* contains elaborate tissue folds [57], while the bulbus in *C. argus* has longitudinal ridges [52]. It has been suggested that these structures might support blood flow separation during cardiac passage [6,52,57]. Evidence of blood flow separation in fish with these structures has been demonstrated in lungfish [6,58] and *C. argus* [52], and speculated to occur in *A. gigas* [20] based on the absence of branchial O₂ loss.

Our heart rate and blood flow findings indicate that during aquatic hypoxia, P. hypophthalmus exhibits the common tachycardia [59,60] [2, table 6.5] associated with air-breathing as reported in several air-breathing fish species. To our knowledge, the current study comprises the first direct measures of blood flow to an ABO in air-breathing fishes. During hypoxia, there was an increase in cardiac output, but the fraction feeding the CMA and hence the ABO, anastomosis and gut remained more or less constant in hypoxia (56%) compared to normoxia (53%) (under the assumption of comparable flows between VA1 and VA2). This means that the shift from water-breathing (93% aquatic O2 uptake) to air-breathing (100% aerial O2 uptake) did not result in a redistribution of blood flow across the branchial basket to increase perfusion to the ABO, which went against our expectations. A study on the spotted gar (L. oculatus) at 20°C, showed that lung perfusion increased from 5.9 to 12.1 ml min⁻¹ kg⁻¹ in severe hypoxia based on indirect measurements (cardiac output calculations and microspheres distribution) [16]. Furthermore, in that study cardiac output increased from 30.0 to 40.5 ml min⁻¹ kg⁻¹ from normoxia to severe hypoxia) [16].

The lack of redistribution of blood flow in P. hypophthalmus during hypoxia might be explained by the unusual anatomical configuration where blood to the first two gill arches supplies the DA while blood to the third and fourth gill arch supplies the CMA. In severe hypoxia, the entire cardiac output can only be oxygenated by the ABO and hence blood flow to the CMA through gill arch 3 and 4 should be favoured. However, blood would still need to transit the first and second gill arch to supply the muscles and brain with oxygen. The anastomosis allows redistribution between these flows in situations where the recipient capillary beds differ in flow resistance. When air-breathing is favoured, blood is oxygenized by the ABO, which must be associated with a reduced resistance in the CMA system and an increased cardiac output. This reduced peripheral resistance could promote blood flow from the DA into the CMA and the lack of redistribution at the ventral aortas might, therefore, be compensated by the anastomosis. A method to reduce branchial O2 loss would be to shunt blood away from the respiratory surface area of the gills [54,61]. However, such shunting away from the branchial surfaces cannot have occurred to a very large extent in P. hypophthalmus given the continued dominance of aquatic CO₂ excretion in hypoxia. Almost all air-breathing fish must accommodate the effects of mixing of oxygenated blood from the ABO return with the de-oxygenated systemic blood of the venous return. This mixing of blood would reduce the oxygen carried in the arterial blood but would limit branchial O2 loss because

of the reduced blood PO₂, and hence the reduced diffusion gradient to the hypoxic water. The exact resolution of this problem would require blood gas measurements and flow measurements at different locations in the cardiovascular system, which at present is not possible.

Given the structure of the cardiovascular system of airbreathing fish, where oxygenated blood returns to the heart before passing the gills, it has been a general dogma within comparative physiology that branchial O2 loss in severe hypoxia is unavoidable. Numerous studies have investigated isolated factors that might mitigate such loss but very few studies have investigated the extent of oxygen loss in deep hypoxia. The fact that P. hypophthalmus, with its very large gills with such thin epithelia, experiences such modest O2 loss even under the forced hypoxia exposure of a respirometer calls, we believe, the whole idea of oxygen loss in air-breathing fish into question. Furthermore, we argue that this species is likely to show a behavioural response to mitigate even this slight loss in its natural habitat. In conclusion, this dataset suggests a simple solution to the oxygen loss problem posed by the inherited single circulatory system and the adaptations to avoid oxygen loss would already be included in the set necessary for air-breathing. Deep hypoxia would tend to reduce the opercular ventilatory drive. Given the much higher solubility of CO₂ compared to O₂, and the ensuing higher ventilatory and diffusive conductances, oxygen loss is limited much more than CO₂ excretion since the diffusion gradient would reach equilibrium much faster for O2. The net result would be a gradual increase in blood PCO2, which would then give rise to a gradual increase in aerially excreted CO₂, which is exactly the pattern observed. Conceivably, O₂ loss for P. hypophthalmus, might play a bigger role during periods of active swimming such as during migration where loss of ILCM is greatly exaggerated, especially if such migrations coincided with high temperatures, such as those projected under climate change scenarios. However, in the well-mixed river water encountered on such migrations, deep hypoxia is probably rare. It is obviously too early to draw conclusions for all of the more than 400 known air-breathing fish species, but it does seem likely that the evolutionary forces stimulating the development of air-breathing might also include adaptations to prevent oxygen loss.

Ethics. All procedures were conducted according to the guidelines of the Danish Law on Animal Experiments and approved by the Danish Ministry of Food, Agriculture and Fisheries (2016-15-0201-00865).

Data accessibility. The respirometry data used in this manuscript are freely available online from Zenodo (https://doi.org/10.5281/zenodo.8256464 [62]). The data are available for download as an excel file, and all the Acqknowledge files with the raw data acquisition are also available.

Additional data are provided in the electronic supplementary material [63].

Declaration of Al use. We have not used AI-assisted technologies in creating this article.

Authors' contributions. M.L.A.: conceptualization, data curation, formal analysis, investigation, methodology, project administration, validation, visualization, writing-original draft, writing-review and editing; D.N.: data curation, formal analysis, investigation, methodology, visualization, writing-original draft, writing-review and editing; H.L.: data curation, investigation, methodology, resources, visualization, writing—review and editing; D.T.T.H.: funding acquisition, project administration, resources, writing-review and editing; A.I.: data curation, investigation, methodology, validation, writing-original draft, writing-review and editing; D.A.C.: supervision, writing-original draft, writing-review and editing; H.M.: formal analysis, methodology, validation, writing-original draft, writing-review and editing; M.B.: conceptualization, data curation, funding acquisition, investigation, methodology, project administration, resources, supervision, writing-original draft, writingreview and editing.

All authors gave final approval for publication and agreed to be held accountable for the work performed therein.

Conflict of interest declaration. We declare we have no competing interests. Funding. This research was funded by the Danish Council for Independent Research | Natural Sciences (Natur og Univers, Det Frie Forskningsråd; grant no. 0135-00256B).

Acknowledgements. We wish to thank Heidi M. Jensen, Simon Olsen and Claus Wandborg for their invaluable assistance in the animal facility, Louise Thomason for her contribution in mapping the circulatory anatomy and Frank de Paoli for his invaluable assistance with the artificial lungs.

References

Downloaded from https://royalsocietypublishing.org/ on 13 September 2023

- Damsgaard C, Baliga VB, Bates E, Burggren W, McKenzie DJ, Taylor E, Wright PA. 2020 Evolutionary and cardio-respiratory physiology of air-breathing and amphibious fishes. *Acta Physiol.* 228, e13406. (doi:10.1111/apha.13406)
- Graham JB. 1997 Air-breathing fishes: evolution, diversity, and adaptation. San Diego, CA: Academic press.
- Graham JB, Wegner NC. 2010 Breathing air in water and in air: the air-breathing fishes. In Respiratory physiology of vertebrates: life with and without oxygen (ed. GE Nilsson), pp. 174–221. Cambridge, UK: Cambridge University Press.
- Bayley M, Damsgaard C, Thomsen M, Malte H, Wang T. 2018 Learning to air-breathe: the first steps. *Physiology* 34, 14–29. (doi:10.1152/physiol.00028.2018)
- Johansen K. 1970 9 Air breathing in fishes. In Fish physiology (eds WS Hoar, DJ Randall), pp. 361–411.
 San Diego, CA: Academic Press. (doi:10.1016/S1546-5098(08)60134-X)

- Olson KR. 1994 Circulatory anatomy in bimodally breathing fish. *Am. Zool.* 34, 280–288. (doi:10. 1093/icb/34.2.280)
- Ishimatsu A. 2012 Evolution of the cardiorespiratory system in air-breathing fishes. *Aqua-BioSci. Monogr.* 5, 1–28. (doi:10.5047/absm.2012.00501.0001)
- Rahn H. 1966 Aquatic gas exchange: theory. *Respir. Physiol.* 1, 1–12. (doi:10.1016/0034-5687(66)90024-7)
- Rahn H, Howell BJ. 1976 Bimodal gas exchange. In Respiration of amphibious vertebrates (ed. GM Hughes), pp. 271–285. New York, NY: Academic press.
- Singh B. 1976 Balance between aquatic and aerial respiration. In *Respiration of amphibious* vertebrates (ed. GM Hughes), pp. 125–164.
 New York, NY: Academic press.
- Brauner CJ, Val AL. 1996 The interaction between 0₂ and CO₂ exchange in the obligate air breather,
 Arapaima gigas, and the facultative air breather,
 Lipossarcus pardalis. In *Physiology and biochemistry of*

- the fishes of the Amazon (eds AL Val, VMF Almeida-Val, DJ Randall), pp. 101–110. Manaus, Brazil: INPA.
- Gonzalez RJ, Brauner CJ, Wang YX, Richards JG, Patrick ML, Xi W, Matey V, Val AL. 2010 Impact of ontogenetic changes in branchial morphology on gill function in *Arapaima gigas*. *Physiol. Biochem. Zool.* 83, 322–332. (doi:10.1086/648568)
- Brauner CJ, Shartau RB, Damsgaard C, Esbaugh AJ, Wilson RW, Grosell M. 2019 Acid—base physiology and CO₂ homeostasis: regulation and compensation in response to elevated environmental CO₂. In *Fish* physiology (eds M Grosell, PL Munday, AP Farrell, CJ Brauner), pp. 69–132. Cambridge, MA: Academic Press. (doi:10.1016/bs.fp.2019.08.003)
- Pelster B, Wood C, Braz-Mota S, Val A. 2020 Gills and air-breathing organ in O₂ uptake, CO₂ excretion, N-waste excretion, and ionoregulation in small and large pirarucu (*Arapaima gigas*). *J. Comp. Physiol. B* 190, 569–583. (doi:10.1007/s00360-020-01286-1)

- Randall DJ, Cameron JN, Daxboeck C, Smatresk N. 1981 Aspects of bimodal gas exchange in the bowfin, *Amia calva* L. (Actinopterygii: Amiiformes). *Respir. Physiol.* 43, 339–348. (doi:10.1016/0034-5687(81)90114-6)
- Smatresk NJ, Cameron JN. 1982 Respiration and acid—base physiology of the spotted gar, a bimodal breather: I. Normal values, and the response to severe hypoxia. *J. Exp. Biol.* 96, 263–280. (doi:10. 1242/jeb.96.1.263)
- Scott GR, Matey V, Mendoza J-A, Gilmour KM, Perry SF, Almeida-Val VMF, Val AL. 2017 Air breathing and aquatic gas exchange during hypoxia in armoured catfish. J. Comp. Physiol. B 187, 117–133. (doi:10.1007/s00360-016-1024-y)
- Randall DJ, Burggren WW, Farrell AP, Haswell MS.
 1981 The evolution of air breathing in vertebrates.
 Cambridge, UK: Cambridge University Press. (doi:10.
 1017/CB09780511753206)
- Bayley M, Damsgaard C, Cong N, Phuong N, Do H. 2020 Aquaculture of air-breathing fishes. In *Fish physiology* (eds TJ Benfey, AP Farrell, CJ Brauner), pp. 315–353. Cambridge, MA: Academic Press.
- Aaskov ML, Jensen RJ, Skov PV, Wood CM, Wang T, Malte H, Bayley M. 2022 *Arapaima gigas* maintains gas exchange separation in severe aquatic hypoxia but does not suffer branchial oxygen loss. *J. Exp. Biol.* 225, jeb243672. (doi:10.1242/jeb. 243672)
- Brauner CJ, Matey V, Wilson JM, Bernier NJ, Val AL. 2004 Transition in organ function during the evolution of air-breathing; insights from; *Arapaima* gigas, an obligate air-breathing teleost from the Amazon. J. Exp. Biol. 207, 1433. (doi:10.1242/jeb. 00887)
- Phuong LM, Huong DTT, Nyengaard JR, Bayley M. 2017 Gill remodelling and growth rate of striped catfish *Pangasianodon hypophthalmus* under impacts of hypoxia and temperature. *Comp. Biochem. Physiol. A Mol. Integr. Physiol.* 203, 288–296. (doi:10.1016/j.cbpa. 2016.10.006)
- Frommel AY, Kwan GT, Prime KJ, Tresguerres M, Lauridsen H, Val AL, Gonçalves LU, Brauner CJ. 2021 Changes in gill and air-breathing organ characteristics during the transition from water- to air-breathing in juvenile Arapaima gigas. J. Exp. Zool. A Ecol. Integr. Physiol. 335, 801–813. (doi:10.1002/jez.2456)
- 24. Johansen K. 1968 Air-breathing fishes. *Sci. Am.* **219**, 102–111
- Lefevre S, Huong do TT, Wang T, Phuong NT, Bayley M. 2011 Hypoxia tolerance and partitioning of bimodal respiration in the striped catfish (*Pangasianodon hypophthalmus*). Comp. Biochem. Physiol. A Mol. Integr. Physiol. 158, 207–214. (doi:10.1016/j.cbpa.2010.10.029)
- Browman MW, Kramer DL. 1985 Pangasius sutchi (Pangasiidae), an air-breathing catfish that uses the swimbladder as an accessory respiratory organ. Copeia 1985, 994–998.
- 27. Zheng WB, Liu WS. 1988 Morphology and histology of the swimbladder and infrastructure of respiratory

- epithelium in the air-breathing catfish, *Pangasius sutchi* (Pangasiidae). *J. Fish Biol.* **33**, 147–154. (doi:10.1111/j.1095-8649.1988.tb05456.x)
- 28. Van Zalinge N. 2002 Update on the status of the Cambodian inland capture fisheries sector with special reference to the Tonle Sap Great Lake. *Catch Cult.* **8**. 1–5.
- So N, van Houdt JKJ, Volckaert FAM. 2006 Genetic diversity and population history of the migratory catfishes *Pangasianodon hypophthalmus* and *Pangasius bocourti* in the Cambodian Mekong River. *Fish. Sci.* 72, 469–476. (doi:10.1111/j.1444-2906. 2006.01174.x)
- Phuong LM, Huong DTT, Malte H, Nyengaard JR, Bayley M. 2018 Ontogeny and morphometrics of the gills and swim bladder of air-breathing striped catfish *Pangasianodon hypophthalmus*. *J. Exp. Biol*. 221, 3. (doi:10.1242/jeb.168658)
- Lefevre S, Wang T, Huong DTT, Phuong NT, Bayley M. 2013 Partitioning of oxygen uptake and cost of surfacing during swimming in the air-breathing catfish *Pangasianodon hypophthalmus. J. Comp. Physiol. B* 183, 215–221. (doi:10.1007/s00360-012-0701-8)
- Harter TS, Brauner CJ, Matthews PGD. 2017 A novel technique for the precise measurement of CO₂ production rate in small aquatic organisms as validated on aeshnid dragonfly nymphs. *J. Exp. Biol.* 220, 964. (doi:10.1242/jeb.150235)
- Kurita M, Noma S, Ishimatsu A. 2021 Morphology of the respiratory vasculature of the mudskipper Boleophthalmus pectinirostris (Gobiidae: Oxudercinae). J. Morphol. 282, 1557–1568. (doi:10. 1002/jmor.21404)
- Rasmussen AS et al. 2010 High-resolution ex vivo magnetic resonance angiography: a feasibility study on biological and medical tissues. BMC Physiol. 10, 3. (doi:10.1186/1472-6793-10-3)
- Zhou Y-Q, Davidson L, Henkelman RM, Nieman BJ, Foster FS, Lisa XY, Chen XJ. 2004 Ultrasound-guided left-ventricular catheterization: a novel method of whole mouse perfusion for microimaging. *Lab*. *Invest.* 84, 385–389.
- Chabot D, Steffensen JF, Farrell AP. 2016
 The determination of standard metabolic rate in fishes. J. Fish Biol. 88, 81–121. (doi:10.1111/ifb.12845)
- 37. Bates D, Mächler M, Bolker B, Walker S. 2015 Fitting linear mixed-effects models using Ime4. *J. Stat. Softw.* **67**, 48. (doi:10.18637/jss.v067.i01)
- Labouriau R. 2020 postHoc: tools for post-hoc analysis. See https://cran.r-project.org/web/ packages/postHoc/postHoc.pdf.
- Hothorn T, Bretz F, Ag P, Westfall P. 2008
 Simultaneous inference in general parametric models *Biom. J.* 50, 346–363. (doi:10.1002/bimj. 200810425)
- Iversen NK, Wang T, Baatrup E, Crossley II DA. 2014
 The role of nitric oxide in the cardiovascular response to chronic and acute hypoxia in white Leghorn chicken (*Gallus domesticus*). *Acta Physiol. (Oxf.)* 211, 346–357. (doi:10.1111/apha.12286)

- 41. Hughes GM, Singh BN. 1970 Respiration in an airbreathing fish, the climbing perch *Anabas testudineus* Bloch: I. Oxygen uptake and carbon dioxide release into air and water. *J. Exp. Biol.* **53**, 265–280. (doi:10.1242/jeb.53.2.265)
- Graham JB. 1983 The transition to air breathing in fishes: II. Effects of hypoxia acclimation on the bimodal gas exchange of *Ancistrus chagresi* (Loricariidae). *J. Exp. Biol.* 102, 157–173. (doi:10. 1242/jeb.102.1.157)
- Lefevre S, Huong DTT, Ha NTK, Wang T, Phuong NT, Bayley M. 2011 A telemetry study of swimming depth and oxygen level in a *Pangasius* pond in the Mekong Delta. *Aquaculture* 315, 410–413. (doi:10. 1016/j.aquaculture.2011.02.030)
- Damsgaard C, Gam LTH, Tuong DD, Thinh PV, Huong Thanh DT, Wang T, Bayley M. 2015 High capacity for extracellular acid—base regulation in the air-breathing fish *Pangasianodon hypophthalmus*. *J. Exp. Biol.* 218, 1290—1294. (doi:10.1242/jeb. 117671)
- de Moraes MF, Höller S, da Costa OT, Glass ML, Fernandes MN, Perry SF. 2005 Morphometric comparison of the respiratory organs in the South American lungfish *Lepidosiren paradoxa* (Dipnoi). *Physiol. Biochem. Zool.* 78, 546–559. (doi:10.1086/ 430686)
- Perry SF, Gilmour KM. 2002 Sensing and transfer of respiratory gases at the fish gill. *J. Exp. Zool.* 293, 249–263. (doi:10.1002/jez.10129)
- Fritsche R, Axelsson M, Franklin CE, Grigg GG, Holmgren S, Nilsson S. 1993 Respiratory and cardiovascular responses to hypoxia in the Australian lungfish. *Respir. Physiol.* 94, 173–187. (doi:10.1016/0034-5687(93)90046-D)
- Takasusuki J, Fernandes MN, Severi W. 1998
 The occurrence of aerial respiration in *Rhinelepis strigosa* during progressive hypoxia. *J. Fish Biol.* 52, 369–379. (doi:10.1111/j.1095-8649.1998. tb00804.x)
- Hvas M, Damsgaard C, Gam LTH, Huong DTT, Jensen FB, Bayley M. 2016 The effect of environmental hypercapnia and size on nitrite toxicity in the striped catfish (*Pangasianodon hypophthalmus*). *Aquat. Toxicol.* 176, 151–160. (doi:10.1016/j. aquatox.2016.04.020)
- Damsgaard C, Phuong LM, Huong DTT, Jensen FB, Wang T, Bayley M. 2015 High affinity and temperature sensitivity of blood oxygen binding in Pangasianodon hypophthalmus due to lack of chloride—hemoglobin allosteric interaction. Am. J. Physiol. Regul. Integr. Comp. Physiol. 308, R907—R915. (doi:10.1152/ajpregu.00470.2014)
- Damsgaard C et al. 2014 High blood oxygen affinity in the air-breathing swamp eel Monopterus albus. Comp. Biochem. Physiol. A Mol. Integr. Physiol. 178, 102–108. (doi:10.1016/j.cbpa.2014.08. 001)
- Ishimatsu A, Itazawa Y. 1983 Difference in blood oxygen levels in the outflow vessels of the heart of an air-breathing fish, *Channa argus*: do separate blood streams exist in a teleostean heart? *J. Comp. Physiol.* 149, 435–440. (doi:10.1007/BF00690000)

- Ishimatsu A, Itazawa Y, Takeda T. 1979 On the circulatory systems of the snakeheads *Channa* maculata and *C. argus* with reference to bimodal breathing. *Jpn J. Ichthyol.* 26, 167–180.
- 54. Smith DG, Gannon BJ. 1978 Selective control of branchial arch perfusion in an air-breathing Amazonian fish *Hoplerythrinus unitaeniatus*. *Can. J. Zool.* **56**, 959–964. (doi:10.1139/z78-132)
- Fishman AP, DeLaney RG, Laurent P. 1985 Circulatory adaptation to bimodal respiration in the dipnoan lungfish. *J. Appl. Physiol.* 59, 285–294. (doi:10.1152/ jappl.1985.59.2.285)
- Buzete Gardinal MV, Rocha Ruiz TF, Estevan Moron S, Oba Yoshioka ET, Uribe Gonçalves L, Franceschini Vicentini IB, Vicentini CA. 2019 Heart structure in the Amazonian teleost *Arapaima gigas*

Downloaded from https://royalsocietypublishing.org/ on 13 September 2023

- (Osteoglossiformes, Arapaimidae). *J. Anat.* **234**, 327–337. (doi:10.1111/joa.12919)
- Scadeng M, McKenzie C, He W, Bartsch H, Dubowitz DJ, Stec D, St. Leger J. 2020 Morphology of the Amazonian teleost genus *Arapaima* using advanced 3D imaging. *Front. Physiol.* 11, 260. (doi:10.3389/fphys.2020.00260)
- Johansen K, Lenfant C, Hanson D. 1968
 Cardiovascular dynamics in the lungfishes. Z. vgl. Physiol. 59, 157–186. (doi:10.1007/BF00339348)
- Johansen K. 1966 Air breathing in the teleost Symbranchus marmoratus. Comp. Biochem. Physiol. 18, 383–395. (doi:10.1016/0010-406X(66)90196-4)
- 60. Armelin VA, Thomsen MT, Teixeira MT, Florindo LH, Bayley M, Wang T. 2019 Cardiovascular and

- ventilatory interactions in the facultative airbreathing teleost *Pangasianodon hypophthalmus*. *J. Comp. Physiol. B* **189**, 425–440. (doi:10.1007/s00360-019-01225-9)
- 61. Satchell G. 1976 The circulatory system of air-breathing fish. In *Respiration of amphibious vertebrates* (ed. GM Hughes), pp. 105–123. New York, NY: Academic press.
- 62. Aaskov ML. 2023 Data from: Respirometry data [data set]. *Zenodo*. (doi:10.5281/zenodo. 8256464)
- Aaskov ML, Nelson D, Lauridsen H, Huong DTT, Ishimatsu A, Crossley II DA, Malte H, Bayley M. 2023 Do air-breathing fish suffer branchial oxygen loss in hypoxic water? Figshare. (doi:10.6084/m9.figshare.c. 6806614)